

激光冲击强化对激光增材制造 TC4 钛合金组织和性能的影响

陈雪鹏¹, 张凌峰^{1,2*}, 熊毅^{1,2}, 罗高丽¹, 武永丽¹

¹河南科技大学材料科学与工程学院, 河南 洛阳 471023;

²有色金属新材料与先进加工技术省部共建协同创新中心, 河南 洛阳 471023

摘要 通过对激光增材制造(LAM)TC4 钛合金表面进行激光冲击强化(LSP), 对比研究了 LSP 处理对 LAM-TC4 钛合金微观组织、力学性能和断口形貌的影响。LAM-TC4 钛合金的原始组织由大量粗大的 α 板条及一定数量的板条间 β 相构成。经 LSP 处理后, 表层组织在高能冲击波的作用下, 原始粗大的 α 板条破碎细化, 形成了大量位错和形变孪晶, 导致晶格畸变。LSP 处理使 LAM-TC4 钛合金的残余应力由残余拉应力转变成残余压应力。LSP 处理后 LAM-TC4 钛合金表面存在的最大残余压应力为 -190 MPa, 显微硬度提高了 16.5%, 显微硬度随深度的增加而减小。此外, 经 LSP 处理后, LAM-TC4 钛合金的屈服强度和抗拉强度较 LSP 处理前分别提高了 46.3% 和 32.3%, 塑性基本维持不变。LSP 处理可使 LAM-TC4 钛合金获得更好的强度和塑性匹配。

关键词 激光技术; 激光增材制造; 激光冲击强化; 钛合金; 微观组织; 力学性能; 断口形貌

中图分类号 TN249

文献标志码 A

DOI: 10.3788/CJL202249.1602017

1 引言

TC4 钛合金具有比强度高、耐热及耐蚀性好等优点, 在航空领域中被广泛应用^[1-2]。航空装备的不断发展对关键主承力结构提出了大型化、整体化和复杂化等要求^[3]。传统锻造和铸造方法工艺复杂、成材率低、后续加工困难, 难以满足此要求。近年来, 增材制造(AM)技术正成为工程、制造、材料和光学等学科的研究热点^[4]。激光增材制造(LAM)具有数字、设计、制造一体化等优势, 能极大地提高原材料的利用率, 特别适合用于制造钛合金结构件, 已成为提升高性能复杂构件设计与制造能力的核心技术之一^[5-10]。

然而, 在钛合金 LAM 过程中, 熔池与基板之间会存在较大的温度梯度, 导致成形件综合力学性能不佳^[11-13]。为了改善 LAM 钛合金的综合力学性能, 研究者对 LAM 钛合金工艺参数、微观组织开展了大量研究工作。齐振佳等^[14]研究发现, 硼元素对 LAM 钛合金的微观组织具有显著的细化效果。Zhan 等^[15]研究发现, 热处理可以有效地控制和消除 LAM 过程中较大的温度梯度导致的残余应力。Ji 等^[16]研究发现, 可以通过优化工艺参数来消除增材制造产生的宏观缺陷。

激光冲击强化(LSP)是金属零件后处理的一种重

要方法, 利用高功率短脉冲激光作用于材料表面, 使材料表面产生残余压应力和加工硬化层, 具有可控性强、强化效果显著等突出优点^[17]。Martinez 等^[18]研究了 LSP 对激光熔覆 S275 和 316 钢的残余应力的缓解效果, 发现 LSP 处理可以引入显著的压应力。Sun 等^[19]将 LSP 技术应用于 2319 铝合金增材制造中, 发现 LSP 可以细化表面组织, 提高显微硬度和拉伸性能。Shiva 等^[20]比较了激光退火和 LSP 对增材制造的 Ni-Ti 记忆合金的影响, 结果表明, LSP 可以诱导残余压应力, 防止表面裂纹的形成。Guo 等^[21]研究了 LSP 对增材制造 Ti6Al4V 钛合金的影响, 结果表明, LSP 使表层组织得到细化, 延伸率有所提高, 但屈服强度和极限抗拉强度的变化不大。以上研究表明, LSP 技术对拓宽 LAM 材料的应用范围是非常有益的^[22]。目前, 关于 LSP 对 LAM 钛合金的影响研究还较少, 因此, LSP 对 LAM-TC4 钛合金组件微观结构和性能的影响值得深入研究。

本文采取 LSP 处理了 LAM-TC4 钛合金, 系统地研究了 LSP 对 LAM-TC4 组织和性能的影响机制, 期望通过改善 LAM 钛合金表层的力学性能来改善其综合力学性能, 为优化 LAM 钛合金组织及力学性能提供试验依据。

收稿日期: 2021-11-10; 修回日期: 2021-11-12; 录用日期: 2022-01-06

基金项目: 国家自然科学基金(U1804146, 52111530068)

通信作者: *zh_lingfeng@163.com

2 试验步骤

2.1 试验材料与方法

试验所选用的材料是 LAM-TC4 钛合金, 化学成分如表 1 所示。

表 1 LAM-TC4 钛合金的化学成分

Table 1 Chemical compositions of LAM-TC4 alloy

Element	Al	V	Fe	C	Ti
Mass fraction /%	6.25	4.12	0.05	0.01	Bal.

在 LAM-TC4 钛合金试样上, 用 DK7732 型线切割机先切出尺寸为 $40 \text{ mm} \times 12 \text{ mm} \times 1.8 \text{ mm}$ 的板状样, 其几何尺寸如图 1 所示。对板状样依次用 400#~2000# 的砂纸进行手工打磨, 对精磨后的板状样进行超声波清洗, 保证待加工表面的清洁。采用 YS80-R200B 型激光冲击强化设备, 对板状样进行单面 LSP 处理, 图 1 所示白块区为 LSP 区域 ($25 \text{ mm} \times 6 \text{ mm}$), 斜线阴影区域为未 LSP 区, 光斑直径为 3 mm, 激光能量为 7 J, 能量密度为 4.95 GW/cm^2 , 波长为 1064 nm, 脉宽为 20 ns, 搭接率为 50%, 约束层为去离子水, 吸收保护层为黑胶带, 冲击次数为 1。在 LSP 处理后的板状样中心区域, 切出符合拉伸标准的板状试样, 板状拉伸试样的尺寸如图 2 所示, 拉伸试样原始标距为 6 mm, 平行长度为 8 mm。经 LSP 处理后, 在板状样的 LSP 区域与未 LSP 区域分别切出尺寸为 $6.0 \text{ mm} \times 6.0 \text{ mm} \times 1.8 \text{ mm}$ 的块状试样。

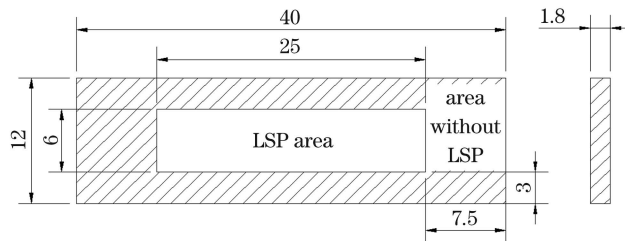


图 1 板状样尺寸

Fig. 1 Dimension of plate sample

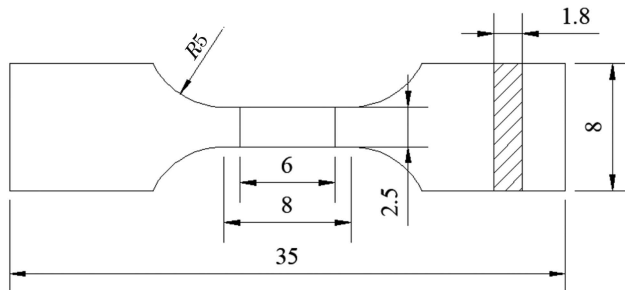


图 2 拉伸试样尺寸

Fig. 2 Dimension of tensile sample

2.2 显微结构表征与性能测试

制备 LSP 与未 LSP 的块状试样的金相, 通过粗抛和细抛将其制成镜面, 之后再用清水冲洗干净, 用体积比为 2:5:43 的氢氟酸、硝酸和蒸馏水配制而成的腐蚀剂进行腐蚀处理, 最后用 OLYMPUS PMG3 型光学

显微镜(OM)进行微观组织观察。

用不同型号的砂纸将 LSP 与未 LSP 的块状试样手工打磨至 $50 \mu\text{m}$ 厚, 之后用 Gatan 691 离子减薄仪减薄, 冲裁得到尺寸为 $\phi 3 \text{ mm}$ 的透射样, 采用 JEM-2010 型高分辨透射电镜(TEM)进行组织结构分析, 加速电压为 200 kV。

使用 D8 ADVANCE 型 X 射线衍射(XRD)分析仪分别对 LSP 与未 LSP 的块状试样进行测试, 采用 Cu-K α 射线, 加速电压为 40 kV, 采用步进扫描模式, 扫描速度为 $2^\circ/\text{min}$, 步长为 0.02° , 扫描角度为 $30^\circ \sim 90^\circ$ 。

用 X-350A 型 X 射线应力分析仪测量 LSP 前、后 LAM-TC4 钛合金试样距表层不同深度处的残余应力, 应力分析仪参数选择如下: Cu K α 射线, X 射线管电压为 27 kV, 电流为 7 mA, 衍射晶面为 $\alpha(213)$ 。用 MH-3 型显微硬度计在 LSP 与未 LSP 的块状试样表面和深度方向上进行硬度测试, 为了减少测量误差, 每个深度方向测量 5 个点的显微硬度, 计算出平均值作为显微硬度值。硬度测试点轨迹如图 3 所示, 施加载荷为 0.98 N, 加载时间为 10 s。

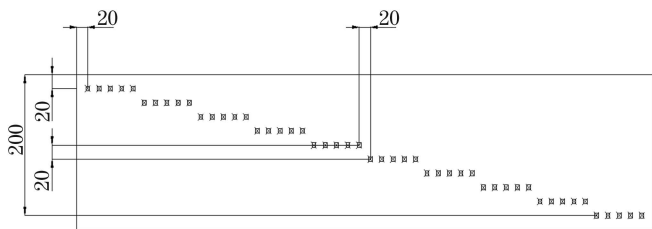


图 3 硬度轨迹图

Fig. 3 Hardness trajectory diagram

采用 Instron 5587 型拉伸试验机测试拉伸性能, 拉伸速度为 0.5 mm/min , 并借助 JSM-IT200 型扫描电子显微镜对 LSP 与未 LSP 的 LAM-TC4 钛合金拉伸样的断口形貌进行分析, 加速电压为 20 kV。

3 试验结果与分析

3.1 LSP 前、后 LAM-TC4 钛合金的 OM 微观组织形貌

LAM 合金的组织特征与激光束作用下金属材料的热过程密切相关^[23]。在 LAM 过程中, 存在多层多道熔覆沉积热效应, 其会对已沉积层产生往复加热/冷却热影响, 直接决定了 LAM 合金晶粒形貌和微观组织与传统锻件明显不同^[3]。图 4(a)给出了 LAM-TC4 钛合金的金相组织形貌, 可见其宏观组织由呈外延生长的粗大 β 柱状胞晶构成, 晶内微观组织是由大量的 α 板条及一定量的板条间 β 相组成, 箭头所指为粗大的 β 柱状晶晶界^[23]。形成这种组织特征的原因是, 高温凝固时, 外延初生 β 柱状枝晶生长, 在往复的加热/冷却过程中快速地发生 β 相到 α 相的固态相变, 同时大量的初生 α 相继续生长成细长的板条状^[24-26]。图 4(b)为 LSP 后的金相组织形貌, 与 LSP 前相比, 原始粗大的 β 柱状晶晶界变得不明显, α 板条更细小。

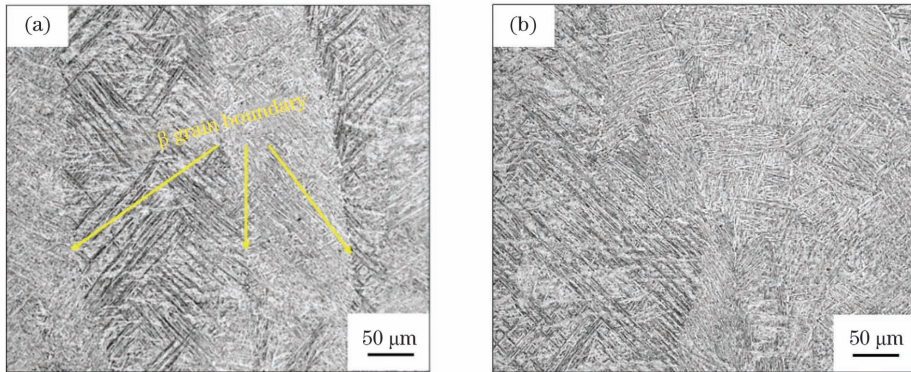


图 4 LSP 前后的 LAM-TC4 钛合金的 OM 微观组织形貌。(a)LSP 前;(b)LSP 后

Fig. 4 OM microstructure morphologies of LAM-TC4 titanium alloy before and after LSP. (a) Before LSP; (b) after LSP

3.2 LSP 前、后 LAM-TC4 钛合金的 TEM 微观组织形貌

通过透射电镜观察可以更好地了解 LSP 前、后 LAM-TC4 的微观组织演变。图 5 为 LSP 前、后 LAM-TC4 钛合金的 TEM 图像及选区电子衍射花样。其中,图 5(a)所示为 LSP 前试样的 TEM 照片,可以看出,在由片状 α 相和残余 β 相构成的基体中几乎没有位错。图 5(b)~(f)所示为 LSP 后试样的 TEM 照片,从图 5(b)中可以看出,粗大 α 板条破碎细

化,这归因于 LSP 诱导的各种位错结构发展形成了(亚)晶粒^[27]。从图 5(c)、(d)中可以看出, α 板条中产生了形变孪晶,位错密度大幅增加,形成了位错网和位错缠结,相界处产生了胞状位错结构^[28]。图 5(e)、(f)为形变孪晶的明场像与暗场像,可以看出, α 板条上存在由大量位错和与形变孪晶交互作用产生的高密度位错缠结。通过对图 5(f)中的区域进行选区电子衍射斑点标定[图 5(f)右上角],可确定其为形变孪晶,孪晶面为{0002}。

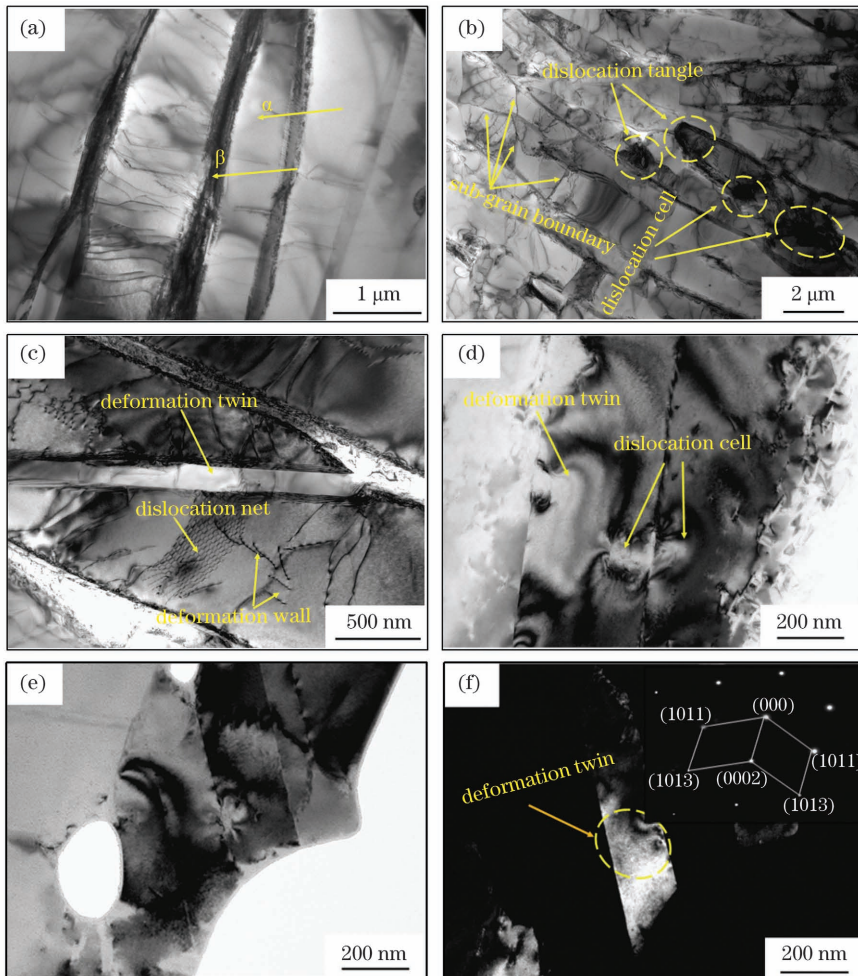


图 5 LSP 前后的 LAM-TC4 钛合金的 TEM 微观组织形貌。(a)LSP 前;(b)~(f)LSP 后

Fig. 5 TEM microstructure morphologies of LAM-TC4 titanium alloy before and after LSP. (a) Before LSP; (b)–(f) after LSP

3.3 LSP 前、后 LAM-TC4 钛合金的 XRD 图谱

图 6 为 LSP 前、后 LAM-TC4 钛合金表面的 XRD 衍射图。从图 6(a)可以看出,其主要物相为六方最密堆积(HCP) α -Ti,经 LSP 处理后,XRD 图谱中没有出现新的衍射峰,即无相变。从衍射峰局部 $34^\circ \sim 42^\circ$ 的放大图[图 6(b)]可以看出, $\alpha(100)$ 和 $\alpha(002)/\beta(110)$ 的衍射峰强度增大,说明经过 LSP 处理后,这些晶面

上出现了变形织构^[29],经 LSP 处理后半峰全宽明显增大,试样晶粒细化至 39.9 nm。衍射峰宽化是晶粒细化和微观应变共同作用的结果^[30]。此外,还可以看到,LSP 后衍射峰的位置略向右偏移,这是由于在 LSP 过程中,LAM-TC4 钛合金表面在高能冲击波作用下产生了较大的残余压应力,引起了晶格畸变和晶面收缩^[31-32]。这也与 Guo 等^[21]的研究结果吻合。

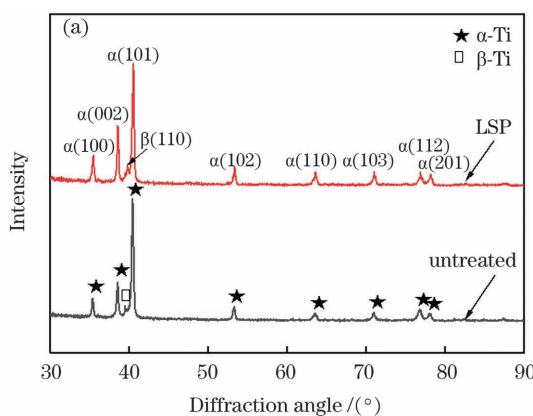


图 6 LSP 前后的 LAM-TC4 钛合金的 XRD 图谱。(a) $30^\circ \sim 90^\circ$; (b) $34^\circ \sim 42^\circ$

Fig. 6 XRD patterns of LAM-TC4 titanium alloy before and after LSP. (a) $30^\circ \sim 90^\circ$; (b) $34^\circ \sim 42^\circ$

3.4 LSP 对 LAM-TC4 钛合金性能的影响

图 7 为 LSP 前、后 LAM-TC4 钛合金不同深度处的残余应力分布图。可以看到,在 LSP 前,LAM-TC4 钛合金表层存在残余拉应力。残余拉应力是热应力和相变应力竞争的结果,其中前者有利于压应力的形成,后者有利于拉应力的形成^[33]。由此可以推断,在 LAM 过程中, β 相到 α 相的固态相变产生的拉应力大于高温度梯度产生的压应力,导致原始样中存在残余拉应力,在 $140 \mu\text{m}$ 深度处产生的最大拉应力为 210 MPa。经 LSP 处理后,在 LAM-TC4 钛合金表层形成了残余压应力,最大值为 -190 MPa ,残余压应力的影响深度为 $180 \mu\text{m}$ 。残余压应力是塑性变形和体积限制的组合作用结果^[34]。LSP 高能冲击波使合金表层发生严重的塑性变形,诱导表层形成残余应力场^[35-36]。距离表面越远,残余压应力值越小,这与激光

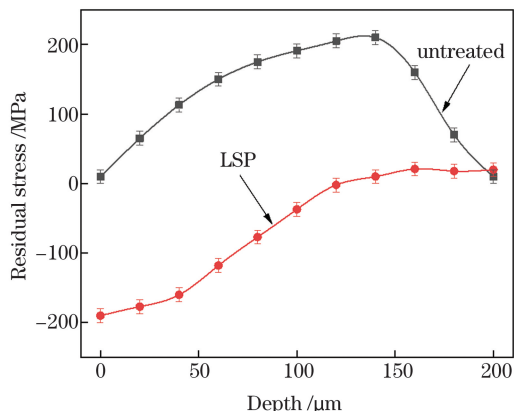
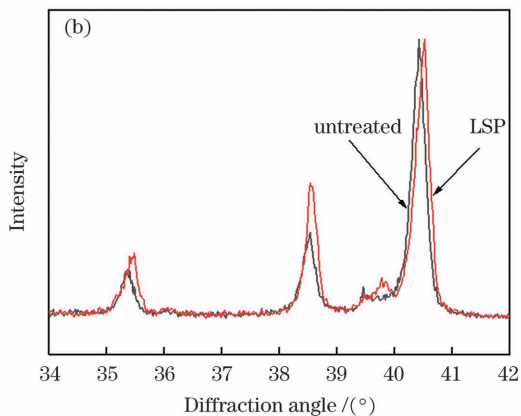


图 7 LSP 前后的 LAM-TC4 钛合金在不同深度处的残余应力

Fig. 7 Residual stress at different depths of LAM-TC4 titanium alloy before and after LSP

冲击波能量随着深度的增加而逐渐衰减有关。这与 Yan 等^[37]的发现一致。

图 8 为 LSP 前、后 LAM-TC4 钛合金表面和深度方向上的显微硬度分布。结果表明,LSP 提高了 LAM-TC4 钛合金试样表面的显微硬度。其中,LSP 前 LAM-TC4 钛合金表面和深度方向上的显微硬度值大致相同,为 326.7 HV。经过 LSP 后,试样表面的显微硬度值显著提高,达到最大值 380.7 HV,提升幅度为 16.5%。显微硬度的提高是位错、形变孪晶和细晶强化等共同作用的结果^[38]。经过 LSP 处理后,LAM-TC4 钛合金表面发生塑性变形,产生大量的位错缠结,阻碍位错的运动,导致表面硬化^[14]。同时,在高能冲击波作用下, α 相结构被破坏并得到细化,有效提升了表面硬度。

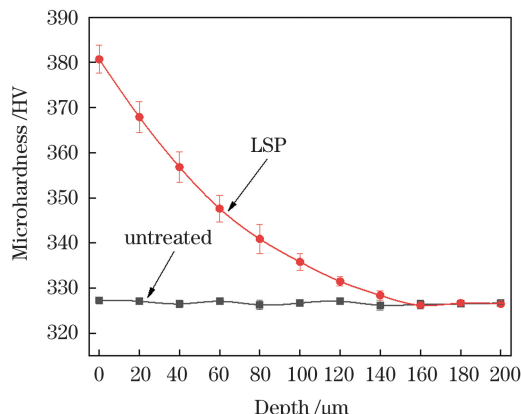


图 8 LSP 前后的 LAM-TC4 钛合金在深度方向上的显微硬度分布

Fig. 8 Microhardness distribution in depth direction of LAM-TC4 titanium alloy before and after LSP

与锻造材料相比,增材制造 TC4 的平均屈服强度和极限抗拉强度略低,塑性相似^[39]。LSP 前、后 LAM-TC4 钛合金的拉伸性能如图 9 所示。可以看出,LSP 前的 LAM-TC4 钛合金的屈服强度为 720 MPa,抗拉强度为 940 MPa,伸长率为 15.5%。LSP 处理一次后,LAM-TC4 钛合金的屈服强度为 1053 MPa,抗拉强度为 1244 MPa,断后伸长率为 15.0%。屈服强度和抗拉强度均有显著提升,断后伸长率基本维持不变。可见 LSP 处理可以消除增材制造引起的负面影响,并提高样品的拉伸性能。经 LSP 处理后,LAM-TC4 钛合金表面发生严重塑性变形,形成高幅值残余压应力,可以抑制裂纹的产生与扩展,使强度增大^[40]。LSP 处理使 LAM-TC4 钛合金表层产生细晶强化,而内部粗晶组织仍具有很高的拉伸应变

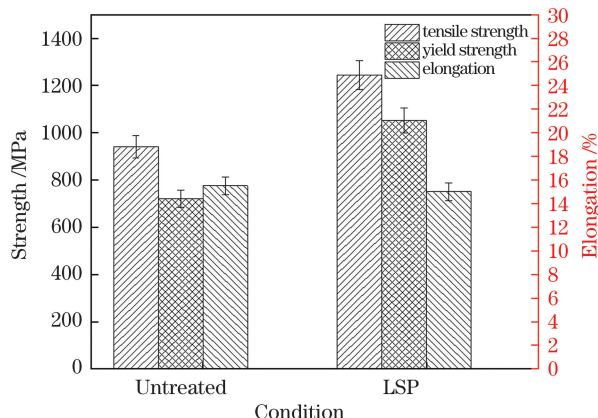


图 9 LSP 前后的 LAM-TC4 钛合金的拉伸性能

Fig. 9 Tensile properties of LAM-TC4 titanium alloy before and after LSP

和加工硬化能力,表层结构可能产生的应变集中和早期颈缩得到有效抑制^[41]。晶粒细化提高材料的强度是基于晶界的影响,晶界会阻碍位错运动,增加位错穿过晶界和从一个晶粒移动到另一个晶粒的难度^[21]。研究表明,细晶细化到纳米尺度后,经典位错活动不再存在,纳米晶粒尺寸小,没有位错滑移的空间^[42],塑性变形的方式变为晶粒旋转和晶界滑动^[43-45]。LSP 处理使 LAM-TC4 钛合金表层组织产生大量形变孪晶,研究发现,孪晶界可以提供位错成核位置,作为位错发射源,提供了更多的可移动位错,使晶体取向有利于晶粒间的协调变形,从而有效地增韧材料,提高材料的塑性^[46-47]。在这些因素的综合作用下,LAM-TC4 钛合金经 LSP 处理后获得了更佳的强度和塑性匹配。

3.5 LSP 前、后 LAM-TC4 钛合金的拉伸断口形貌

LSP 前、后 LAM-TC4 钛合金的拉伸断口形貌如图 10 所示。断口形貌以深等轴韧窝为主,断裂机制均为典型的韧性断裂。图 10(a)、(b) 为未经 LSP 处理的 LAM-TC4 钛合金表层和心部的拉伸断口形貌,可以看出,表层拉伸断口包含大量大小不一的韧窝和少量孔洞,与心部断口形貌无明显区别。图 10(c)、(d) 为经 LSP 处理的 LAM-TC4 钛合金表层和心部的拉伸断口形貌,与图 10(a)、(b) 中的韧窝相比,可以看出,经过 LSP 处理后,表层强化区域的韧窝小且浅,韧窝分布均匀,这是由于表层晶粒在高能冲击波的作用下充分破碎,晶粒细化;经 LSP 处理的钛合金心部断口韧窝与未经 LSP 处理的钛合金心部断口韧窝相比也较细且浅,但其变化没有表层强化区明显,这是由于心部所选区域也受到一定冲击波影响。

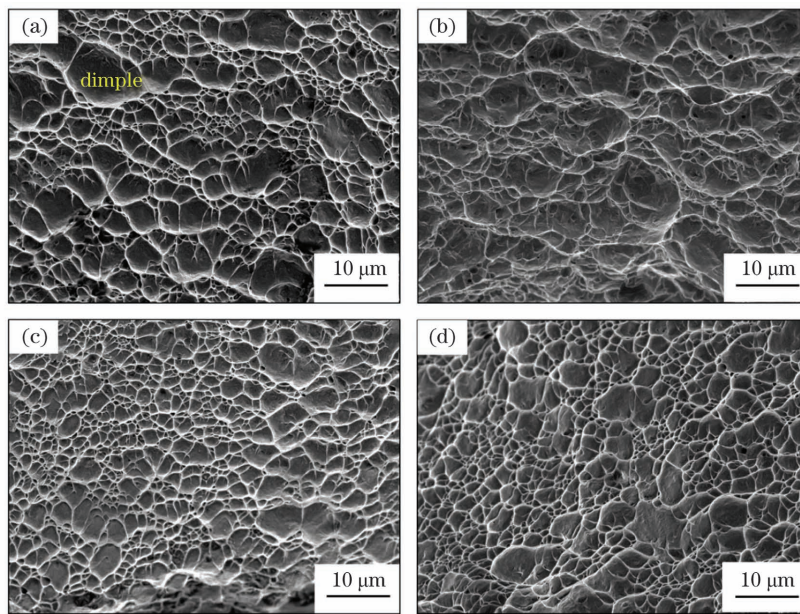


图 10 LSP 前后的 LAM-TC4 钛合金的拉伸断口形貌。(a)LSP 前试样的表层断口形貌;(b)LSP 前试样的心部断口形貌;(c)LSP 后试样的表层断口形貌;(d)LSP 后试样的心部断口形貌

Fig. 10 Tensile fracture morphologies of LAM-TC4 titanium alloy before and after LSP. (a) Surface fracture morphology of sample before LSP; (b) heart fracture morphology of sample before LSP; (c) surface fracture morphology of sample after LSP; (d) heart fracture morphology of sample after LSP

4 结 论

采用LSP对LAM-TC4钛合金进行表面处理,系统地研究了LSP对LAM-TC4钛合金组织演变和性能的影响,得到以下结论。

1)LSP处理使LAM-TC4钛合金表层发生严重的塑性变形,表层基体中产生大量形变孪晶,位错密度大幅增加,各种位错结构交互作用,形成了(亚)晶粒,从而晶粒细化。

2)LSP处理后LAM-TC4钛合金表面存在最大残余应力(-190 MPa),试样表面的显微硬度值显著提高,达到最大值380.7 HV。残余应力和显微硬度值随着深度的增加而减小。

3)LSP处理后LAM-TC4钛合金的屈服强度和抗拉强度与原始相比分别提高了46.3%和32.3%,塑性基本维持不变,断口形貌仍以深等轴韧窝为主,合金获得了更好的强度和塑性匹配。

参 考 文 献

- [1] 张升,桂睿智,魏青松,等.选择性激光熔化成形TC4钛合金开裂行为及其机理研究[J].机械工程学报,2013,49(23):21-27.
Zhang S, Gui R Z, Wei Q S, et al. Cracking behavior and formation mechanism of TC4 alloy formed by selective laser melting[J]. Journal of Mechanical Engineering, 2013, 49(23): 21-27.
- [2] 原国森,兗利鹏,韩艳艳.钛合金的应用进展[J].热加工工艺,2017,46(4):13-16.
Yuan G S, Yan L P, Han Y Y. Application progress of titanium alloy[J]. Hot Working Technology, 2017, 46(4): 13-16.
- [3] 张纪奎,孔祥艺,马少俊,等.激光增材制造高强高韧TC11钛合金力学性能及航空主承力结构应用分析[J].航空学报,2021,42(10):525430.
Zhang J K, Kong X Y, Ma S J, et al. Laser additive manufactured high strength-toughness TC11 titanium alloy: mechanical properties and application in airframe load-bearing structure[J]. Acta Aeronautica et Astronautica Sinica, 2021, 42(10): 525430.
- [4] 顾冬冬,张红梅,陈洪宇,等.航空航天高性能金属材料构件激光增材制造[J].中国激光,2020,47(5):0500002.
Gu D D, Zhang H M, Chen H Y, et al. Laser additive manufacturing of high-performance metallic aerospace components[J]. Chinese Journal of Lasers, 2020, 47(5): 0500002.
- [5] 王华明.高性能大型金属构件激光增材制造:若干材料基础问题[J].航空学报,2014,35(10):2690-2698.
Wang H M. Materials' fundamental issues of laser additive manufacturing for high-performance large metallic components[J]. Acta Aeronautica et Astronautica Sinica, 2014, 35(10): 2690-2698.
- [6] 张家莲,李发亮,张海军.选区激光熔化技术制备金属材料研究进展[J].激光与光电子学进展,2019,56(10):100003.
Zhang J L, Li F L, Zhang H J. Research progress on preparation of metallic materials by selective laser melting[J]. Laser & Optoelectronics Progress, 2019, 56(10): 100003.
- [7] 刘江伟,国凯,王广春,等.金属基材料激光增材制造材料体系与发展现状[J].激光杂志,2020,41(3):6-16.
Liu J W, Guo K, Wang G C, et al. Materials and development states of laser additive manufactured metal-based alloys [J]. Laser Journal, 2020, 41(3): 6-16.
- [8] Gu D D, Meiners W, Wissenbach K, et al. Laser additive manufacturing of metallic components: materials, processes and mechanisms[J]. International Materials Reviews, 2012, 57(3): 133-164.
- [9] Donoghue J, Sidhu J, Wescott A, et al. Integration of deformation processing with additive manufacture of Ti-6Al-4V components for improved β grain structure and texture[M]// TMS 2015 144th Annual Meeting & Exhibition. Cham: Springer, 2016: 437-444.
- [10] 杨永强,陈杰,宋长辉,等.金属零件激光选区熔化技术的现状及进展[J].激光与光电子学进展,2018,55(1):011401.
Yang Y Q, Chen J, Song C H, et al. Current status and progress on technology of selective laser melting of metal parts [J]. Laser & Optoelectronics Progress, 2018, 55(1): 011401.
- [11] 黄卫东,林鑫,陈静.激光立体成形:高性能致密金属零件的快速自由成形[M].西安:西北工业大学出版社,2007:126-142.
Huang W D, Lin X, Chen J. Laser stereoscopic forming: rapid free forming of high-performance dense metal parts[M]. Xi'an: Northwestern Polytechnical University Press, 2007: 126-142.
- [12] Zhu Y Y, Li J, Tian X J, et al. Microstructure and mechanical properties of hybrid fabricated Ti-6.5Al-3.5Mo-1.5Zr-0.3Si titanium alloy by laser additive manufacturing[J]. Materials Science and Engineering: A, 2014, 607: 427-434.
- [13] 张兴寿,王勤英,郑淮北,等.激光增材制造合金材料残余应力及应力腐蚀研究现状[J].激光与光电子学进展,2022,59(13):1300001.
Zhang X S, Wang Q Y, Zheng H B, et al. Current situation of study on residual stress and stress corrosion of alloy materials in laser additive manufacturing [J]. Laser & Optoelectronics Progress, 2022, 59(13): 1300001.
- [14] 齐振佳,张晓星,王豫跃,等.硼对激光增材制造TC4微观组织及力学性能的影响[J].中国激光,2020,47(6):0602002.
Qi Z J, Zhang X X, Wang Y Y, et al. Effect of B on microstructure and tensile properties of laser additive manufactured TC4 alloy[J]. Chinese Journal of Lasers, 2020, 47(6): 0602002.
- [15] Zhan Y, Xu H X, Du W Q, et al. Research on the influence of heat treatment on residual stress of TC4 alloy produced by laser additive manufacturing based on laser ultrasonic technique[J]. Ultrasonics, 2021, 115: 106466.
- [16] Ji L, Lu J P, Tang S Y, et al. Research on mechanisms and controlling methods of macro defects in TC4 alloy fabricated by wire additive manufacturing[J]. Materials, 2018, 11(7): 1104.
- [17] Liao Y L, Ye C, Cheng G J. A review: warm laser shock peening and related laser processing technique[J]. Optics & Laser Technology, 2016, 78: 15-24.
- [18] Martinez H A, Francis J A, Stevens N P C. An assessment of residual stress mitigation strategies for laser clad deposits[J]. Materials Science and Technology, 2016, 32(14): 1484-1494.
- [19] Sun R J, Li L H, Zhu Y, et al. Microstructure, residual stress and tensile properties control of wire-arc additive manufactured 2319 aluminum alloy with laser shock peening[J]. Journal of Alloys and Compounds, 2018, 747: 255-265.
- [20] Shiva S, Palani I A, Paul C P, et al. Comparative investigation on the effects of laser annealing and laser shock peening on the as-manufactured Ni-Ti shape memory alloy structures developed by laser additive manufacturing [M]//Dixit U S, Joshi S N, Davim P. Application of lasers in manufacturing. Lecture notes on multidisciplinary industrial engineering. Singapore: Springer, 2019: 1-20.
- [21] Guo W, Sun R J, Song B W, et al. Laser shock peening of laser additive manufactured Ti_6Al_4V titanium alloy[J]. Surface and Coatings Technology, 2018, 349: 503-510.
- [22] Hackel L, Rankin J R, Rubenchik A, et al. Laser peening: a tool for additive manufacturing post-processing [J]. Additive Manufacturing, 2018, 24: 67-75.
- [23] 林鑫,黄卫东.高性能金属构件的激光增材制造[J].中国科学:信息科学,2015,45(9):1111-1126.

- Lin X, Huang W D. Laser additive manufacturing of high-performance metal components [J]. Scientia Sinica (Informationis), 2015, 45(9): 1111-1126.
- [24] 钦兰云, 吴佳宝, 王伟, 等. 激光增材制造 Ti-6Al-2Mo-2Sn-2Zr-2Cr-2V 钛合金组织与疲劳性能研究[J]. 中国激光, 2020, 47(10): 1002008.
- Qin L Y, Wu J B, Wang W, et al. Microstructures and fatigue properties of Ti-6Al-2Mo-2Sn-2Zr-2Cr-2V titanium alloy fabricated using laser deposition manufacturing [J]. Chinese Journal of Lasers, 2020, 47(10): 1002008.
- [25] Zhu Y Y, Tian X J, Li J, et al. Microstructure evolution and layer bands of laser melting deposition Ti-6.5Al-3.5Mo-1.5Zr-0.3Si titanium alloy [J]. Journal of Alloys and Compounds, 2014, 616: 468-474.
- [26] Ren H S, Tian X J, Liu D, et al. Microstructural evolution and mechanical properties of laser melting deposited Ti-6.5Al-3.5Mo-1.5Zr-0.3Si titanium alloy [J]. Transactions of Nonferrous Metals Society of China, 2015, 25(6): 1856-1864.
- [27] Wen M, Liu G, Gu J F, et al. Dislocation evolution in titanium during surface severe plastic deformation [J]. Applied Surface Science, 2009, 255(12): 6097-6102.
- [28] 眭垚旭, 贾蔚菊, 赵恒章, 等. 激光冲击对 Ti834 合金残余应力及显微组织的影响[J]. 稀有金属材料与工程, 2019, 48(11): 3535-3540.
- Zan Y X, Jia W J, Zhao H Z, et al. Effect of laser shock processing on residual stress and microstructure of Ti834 titanium alloy[J]. Rare Metal Materials and Engineering, 2019, 48(11): 3535-3540.
- [29] Pan X L, Wang X D, Tian Z, et al. Effect of dynamic recrystallization on texture orientation and grain refinement of Ti₆Al₄V titanium alloy subjected to laser shock peening [J]. Journal of Alloys and Compounds, 2021, 850: 156672.
- [30] Kheradmandfar M, Kashani-Bozorg S F, Kang K H, et al. Simultaneous grain refinement and nanoscale spinodal decomposition of β phase in Ti-Nb-Ta-Zr alloy induced by ultrasonic mechanical impacts [J]. Journal of Alloys and Compounds, 2018, 738: 540-549.
- [31] Sundar R, Sudha C, Rai A K, et al. Effect of laser shock peening on the microstructure, tensile and heat transport properties of alloy D9 [J]. Lasers in Manufacturing and Materials Processing, 2020, 7(3): 259-277.
- [32] Dhakal B, Swaroop S. Effect of laser shock peening on mechanical and microstructural aspects of 6061-T6 aluminum alloy [J]. Journal of Materials Processing Technology, 2020, 282: 116640.
- [33] Liu Y, Qin S W, Zhang J Z, et al. Influence of transformation plasticity on the distribution of internal stress in three water-quenched cylinders[J]. Metallurgical and Materials Transactions A, 2017, 48(10): 4943-4956.
- [34] Yin M G, Cai Z B, Li Z Y, et al. Improving impact wear resistance of Ti-6Al-4V alloy treated by laser shock peening[J]. Transactions of Nonferrous Metals Society of China, 2019, 29 (7): 1439-1448.
- [35] 焦清洋, 韩培培, 陆莹, 等. 激光冲击强化对 TA15 钛合金残余应力和力学性能的影响[J]. 塑性工程学报, 2021, 28(3): 146-152.
- Jiao Q Y, Han P P, Lu Y, et al. Effect of laser shock peening on residual stress and mechanical properties of TA15 titanium alloy[J]. Journal of Plasticity Engineering, 2021, 28(3): 146-152.
- [36] Lu Y, Sun G F, Wang Z D, et al. The effects of laser peening on laser additive manufactured 316L steel[J]. The International Journal of Advanced Manufacturing Technology, 2020, 107(5/6): 2239-2249.
- [37] Yan X L, Wang F, Deng L M, et al. Effect of laser shock peening on the microstructures and properties of oxide-dispersion-strengthened austenitic steels [J]. Advanced Engineering Materials, 2018, 20(3): 1700641.
- [38] Liu Y G, Li M Q, Liu H J. Surface nanocrystallization and gradient structure developed in the bulk TC4 alloy processed by shot peening[J]. Journal of Alloys and Compounds, 2016, 685: 186-193.
- [39] Wang F D, Williams S, Colegrove P, et al. Microstructure and mechanical properties of wire and arc additive manufactured Ti-6Al-4V[J]. Metallurgical and Materials Transactions A, 2013, 44(2): 968-977.
- [40] Wu L J, Luo K Y, Liu Y, et al. Effects of laser shock peening on the micro-hardness, tensile properties, and fracture morphologies of CP-Ti alloy at different temperatures [J]. Applied Surface Science, 2018, 431: 122-134.
- [41] Lu K, Lu L, Suresh S. Strengthening materials by engineering coherent internal boundaries at the nanoscale[J]. Science, 2009, 324(5925): 349-352.
- [42] Dai S J, Zhu Y T, Huang Z W. Microstructure evolution and strengthening mechanisms of pure titanium with nano-structured surface obtained by high energy shot peening [J]. Vacuum, 2016, 125: 215-221.
- [43] Ke M, Hackney S A, Milligan W W, et al. Observation and measurement of grain rotation and plastic strain in nanostructured metal thin films[J]. Nanostructured Materials, 1995, 5(6): 689-697.
- [44] Hellstern E, Fecht H J, Fu Z, et al. Structural and thermodynamic properties of heavily mechanically deformed Ru and AlRu [J]. Journal of Applied Physics, 1989, 65(1): 305-310.
- [45] Murayama M, Howe J M, Hidaka H, et al. Atomic-level observation of disclination dipoles in mechanically milled, nanocrystalline Fe[J]. Science, 2002, 295(5564): 2433-2435.
- [46] Asaro R J, Suresh S. Mechanistic models for the activation volume and rate sensitivity in metals with nanocrystalline grains and nano-scale twins[J]. Acta Materialia, 2005, 53(12): 3369-3382.
- [47] Wang Y B, Sui M L. Atomic-scale *in situ* observation of lattice dislocations passing through twin boundaries [J]. Applied Physics Letters, 2009, 94(2): 021909.

Effect of Laser Shock Peening on Microstructure and Properties of Laser Additive Manufactured TC4 Titanium Alloy

Chen Xuepeng¹, Zhang Lingfeng^{1,2*}, Xiong Yi^{1,2}, Luo Gaoli¹, Wu Yongli¹

¹School of Materials Science and Engineering, Henan University of Science and Technology, Luoyang 471023, Henan, China;

²Provincial and Ministerial Co-construction of Collaborative Innovation Center for Non-ferrous Metal New Materials and Advanced Processing Technology, Luoyang 471023, Henan, China

Abstract

Objective TC4 titanium alloy is widely used in the aerospace industry due to its high specific strength and good heat and corrosion resistance. Laser additive manufacturing has the advantages of digital design and manufacturing integration, which can greatly improve the utilization rate of raw materials and is particularly suitable for manufacturing the structural parts of titanium alloy. It has become one of the core technologies to enhance the design and manufacturing capability of high-performance complex components. However, during laser additive manufacturing of titanium alloy, there exists a large temperature gradient between the melt pool and the substrate, which results in the poor comprehensive mechanical properties of formed parts. Therefore, it is very important to find a suitable method to improve the comprehensive mechanical properties and extend the service life. Laser shock peening (LSP) is an important method for the post-treatment of metal parts, which uses a high-power short-pulse laser on the surface of the material to produce compressive residual stresses and work hardening layers, and thus it possesses the outstanding advantages of controllability and significant strengthening effect. In this paper, the effect mechanism of LSP on the microstructure and properties of laser additive manufactured TC4 (LAM-TC4) titanium alloy is systematically investigated by adopting the LSP surface treatment. It is expected to first improve the mechanical properties of the surface layer of the LAM-TC4 titanium alloy, then improve the comprehensive mechanical properties, and finally provide an experimental basis for optimizing the microstructure and mechanical properties of LAM-TC4 titanium alloy.

Methods In this work, LSP is first applied to the surface of the LAM-TC4 titanium alloy. Then, the physical phases of block samples before and after LSP are analyzed by the X-ray diffractometer (XRD), and the microstructures of block samples before and after LSP are observed by the optical microscope (OM). The block samples before and after LSP are manually ground to 50 μm thick ones with different types of sandpapers and punched into $\phi 3$ mm discs. Then they are thinned by the Gatan 691 ion thinning instrument, and the microstructure is further investigated using the JEM-2010 transmission electron microscope (TEM). Finally, the mechanical properties and fracture morphologies of the samples before and after LSP are characterized by the X-ray stress analyzer, the microhardness tester, the tensile testing machine, and the scanning electron microscope (SEM).

Results and Discussions The original microstructure of the LAM-TC4 titanium alloy consists of a large number of thick α laths and a certain volume fraction of inter-lath β phases [Fig. 4(a)]. After the LSP treatment, the microstructure of the surface layer is broken and refined by the action of high-energy shock waves [Fig. 5(b)], and a large number of dislocations [Fig. 5(b-d)] and deformation twins [Fig. 5(d)-(f)] are formed. The LSP treatment changes the tensile residual stress of the LAM-TC4 titanium alloy into the compressive residual stress (Fig. 7). After the LSP treatment, the surface of the LAM-TC4 titanium alloy has the maximum compressive residual stress (-190 MPa) (Fig. 7), the microhardness is increased by 16.5% (Fig. 8), and the microhardness decreases with the increase of depth. In addition, after the LSP treatment, the yield strength and tensile strength of LAM-TC4 titanium alloy are increased by 46.3% and 32.3%, respectively, compared with those of the original sample, and the plasticity remains basically unchanged (Fig. 9). The fracture morphologies of the LAM-TC4 titanium alloy before and after LSP are mainly composed of deep equiaxed dimples, and the fracture mechanism is typical of ductile fracture (Fig. 10).

Conclusions The effect of LSP on the microstructural evolution and properties of the LAM-TC4 titanium alloy is systematically investigated by the surface treatment based on LSP. It is shown that the LSP treatment causes severe plastic deformation in the surface layer of the LAM-TC4 titanium alloy, generates a large number of deformation twins in the surface matrix, the dislocation density increases significantly, and the interaction among various dislocation structures develops to form (sub) grains resulting in grain refinement. The maximum compressive residual stress (-190 MPa) exists on the surface of the LAM-TC4 titanium alloy after the LSP treatment, and the surface microhardness value of the specimen increases significantly, reaching the maximum value of 380.7 HV. Both the residual stress and microhardness

decrease with the increase of depth, and the corresponding values decrease with the increase of distance from the surface layer. The yield strength and tensile strength of the LAM-TC4 titanium alloy after the LSP treatment are increased by 46.3% and 32.3%, respectively, compared with those of the original sample, while the plasticity remains basically unchanged. The fracture morphology is still dominated by deep equiaxial dimples, and the alloy obtains a better match between strength and plasticity.

Key words laser technique; laser additive manufacturing; laser shock peening; titanium alloy; microstructure; mechanical properties; fracture morphology